

論文内容の要旨

Direct Measurement of the Breakout Reaction $^{11}\text{C}(\alpha, p)^{14}\text{N}$
in Explosive Hydrogen-Burning Process

(爆発的水素燃焼過程における抜け出し反応 $^{11}\text{C}(\alpha, p)^{14}\text{N}$ の直接測定)

早川勢也

We have studied the $^{11}\text{C}(\alpha, p)^{14}\text{N}$ reaction which bridges the pp -chain elements to the CNO-cycle elements in addition to the well-known triple- α process, and is important for the nucleosynthesis to the heavier nuclei. In high-temperature ($T \sim 10^8$ – 10^9 K) hydrogen-burning processes taking place in this bridging region and the following proton-rich region up to mass number $A \sim 40$, such (α, p) reactions could bypass the slower β -decays (αp -process). The $^{11}\text{C}(\alpha, p)^{14}\text{N}$ reaction could especially play an important roll in the hot pp -chains in metal-poor stars or in the neutrino-induced rapid proton-capture process (νp -process) in the very early epoch of type II supernovae. This process is expected to explain the origin of the isolated stable neutron-deficient nuclei (p -nuclei) around mass number $A = 100$. However, most of such (α, p) reaction rates in the proton-rich region are still not well known due to experimental difficulties, such as small cross sections, identification of the final states, etc. The $^{11}\text{C}(\alpha, p_0)^{14}\text{N}$ reaction rates in available compilations are only based on the time-reversal reaction studies done by the activation method, which thus do not provide any information on the transitions to the excited states of ^{14}N . For the total reaction rate, one might adopt the Hauser-Feshbach statistical model calculation, but this is not necessarily applicable to such a light nucleus. A direct measurement was desired since it enables us to observe such excited-state transitions and also has an advantage over the activation method in determination of the absolute value of reaction cross sections.

Therefore, we have performed a direct measurement of this reaction as one of the first few successful experiments for the αp -process reactions. We observed the $^{11}\text{C}(\alpha, p)^{14}\text{N}$ reaction

events in a center-of-mass energy range $E_{\text{cm}} = 1.2\text{--}4.5$ MeV by means of the thick target method in inverse kinematics with ^{11}C radioactive beams. The ^{11}C beams were produced by the in-flight technique with CRIB (Center for Nuclear Study Radioactive Ion Beam separator). A $^{11}\text{B}^{3+}$ primary beam at 4.6 MeV/u and with a maximum intensity of 1 pμA was bombarded to a cryogenic ^1H gaseous target with a thickness of 1.2–1.7 mg/cm². The secondary ions were purified by the double achromatic system and the Wien filter of CRIB. By switching the beam-line detectors with different thicknesses in the scattering chamber, we created ^{11}C beams at two different on-target energies 10.1 ± 0.9 MeV and 16.9 ± 0.7 MeV in order to cover a wide energy range. The experimental setup consisted of two beam-line monitors (PPAC: Parallel Plate Avalanche Counter or MCP: MicroChannel Plate detector), a ^4He gaseous target, and ΔE - E position-sensitive silicon detectors at three different angles. We carefully designed the target length (140 mm) and pressure (400 Torr) and the incident beam energy in order to differentiate the ground- and the excited-state transitions in time of flight between the first PPAC and the silicon telescopes.

Although the separations in time between different transitions were not very clear, we successfully extracted the mixing ratios of the numbers of events of each transition by Gaussian fittings to the time spectra at every center-of-mass energy bin. since the angular distributions did not show strong dependence on angle, we made isotropy approximations although we had limited angular range of measurement.

In Fig. 1, the obtained astrophysical S -factors for $^{11}\text{C}(\alpha, p_0)^{14}\text{N}$ (top), $^{11}\text{C}(\alpha, p_1)^{14}\text{N}^*$ (middle) and $^{11}\text{C}(\alpha, p_2)^{14}\text{N}^*$ (bottom) are shown. In the top figure, the previous (α, p_0) S -factors of the fit with a quadratic function with its error (“CF88”, dashed line and hatch), the Padé approximation (“Takacs03”, dotted line) and the Hauser-Feshbach statistical model calculation by the code NON-SMOKER^{WEB} (dashed-dotted line) are shown together. In the middle and the bottom figures, the original Hauser-Feshbach calculations (dashed lines) and the normalized Hauser-Feshbach calculations by the logarithmic least squares method with their errors (solid lines and hatches) are shown. The errors of the CF88 S -factor for (α, p_0) and the Hauser-Feshbach S -factors for (α, p_1) and (α, p_2) are defined as the logarithmic standard deviations from the present experimental data. We confirmed that the present (α, p_0) excited function is eventually consistent with Takacs03. For the whole-energy S -factor of (α, p_0) , we adopted and those of CF88, and Takacs03 below and above the experimental energy range, respectively. For the whole-energy (α, p_1) and the (α, p_2) S -factors, we tentatively used the normalized Hauser-Feshbach ones for the energy ranges out of measurement.

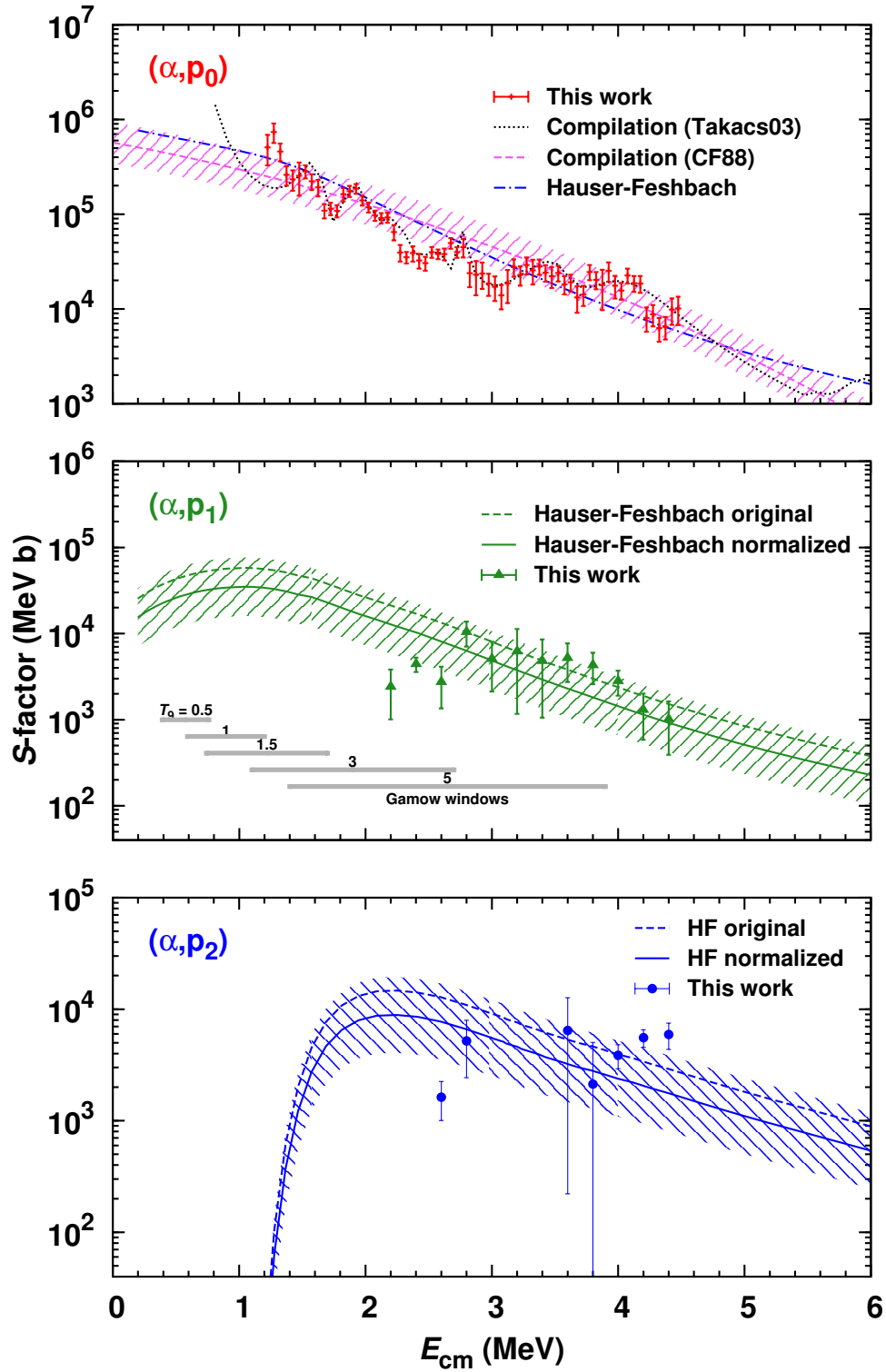


Figure 1: S -factors for $^{11}\text{C}(\alpha, p_0)^{14}\text{N}$ (top), $^{11}\text{C}(\alpha, p_1)^{14}\text{N}^*$ (middle) and $^{11}\text{C}(\alpha, p_2)^{14}\text{N}^*$ (bottom). In the top figure, the present (α, p_0) S -factors (dots with error bars), the fit with a quadratic function with its error (“CF88”, dashed line and hatch), the Padé approximation (“Takacs03”, dotted line) and the Hauser-Feshbach statistical model calculation (dashed-dotted line) are shown. In the middle and the bottom figures, the (α, p_1) and the (α, p_2) S -factors, respectively, of the present experimental data (dots with error bars), the original Hauser-Feshbach calculations (dashed lines) and the normalized Hauser-Feshbach calculations with their errors (solid lines and hatches) are shown. Gamow windows from $T_9 = 0.5$ –5 are also illustrated together as gray bars in the middle figure.

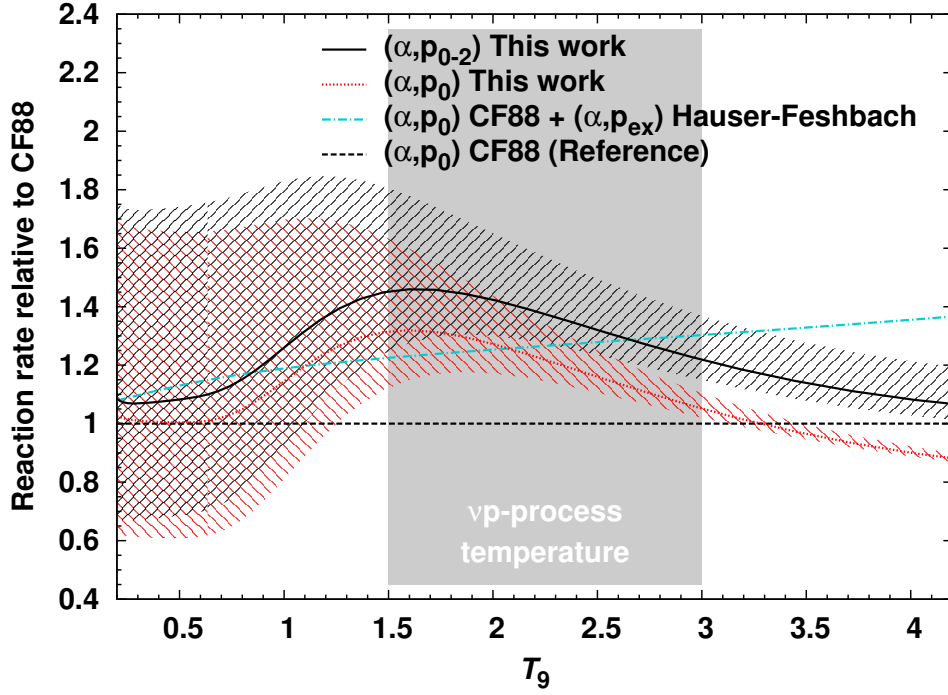


Figure 2: The present (α, p_0) (dotted line) and total (solid line) reaction rates and the previous recommended rate (dashed-dotted line) relative to the CF88 rate (dashed line). The errors of the present rates are drawn in hatches. The temperature range of the νp -process are indicated in gray.

Figure 2 shows the present (α, p_0) (dotted line) and total (solid line) reaction rates and the previous recommended rate (dashed-dotted line) relative to the CF88 rate (dashed line). The errors of the present rates are drawn in hatches. In the νp -process temperature range, shown in the gray area, the present (α, p_0) reaction rate is enhanced from the CF88 rate by 30% at most, mainly due to the resonance at $E_{\text{cm}} = 1.25$ MeV which was not taken into account previously. The contribution from the (α, p_1) and (α, p_2) reaction rate to the total reaction rate is about 15% of the (α, p_0) at most. The error of the total reaction rate is about 25% at $T_9 = 1.5$ and 10% at $T_9 = 3$. We confirmed that the previous total reaction rate is eventually consistent with the present one within its error, and the difference is less than 20%, which could results in no significant change on the stellar models.